

Electronic structure of a metal-insulator interface: Towards a theory of nonreactive adhesion

G. Bordier

Centre d'Études Nucléaires de Saclay, DPE/SPEA, 91191 Gif-sur-Yvette CEDEX, France

C. Noguera

Laboratoire de Physique des Solides, Université de Paris-Sud, 91405 Orsay, France

(Received 18 December 1990; revised manuscript received 29 April 1991)

With the aim of studying metal-insulator adhesion, we have performed an analytical description of the electronic structure of a flat and defectless metal-insulator interface, for both rocksalt and zinc-blende crystallographic structures of the insulator and, respectively, (100) and (110) orientations of the interface. We model the metal by a jellium, and the *AB*-type insulator by a tight-binding Hamiltonian with one atomic orbital per site. A matching procedure involving a Green's-function method yields the local density of states of the metal-induced gap states (MIGS), which are found to be in good agreement with previous numerical estimations on specific materials. By analytically solving the Poisson equation in a self-consistent way, we are able to determine the position of the Fermi level of the whole system for any value of the insulator ionicity. Our results depend upon the density of electrons in the metal, and upon the penetration length and the density of MIGS at midgap. They do not depend much upon the crystallographic structure and orientation of the interface. The two relevant parameters are the Fermi energy of the metal and a ratio that represents the ionocovalent character of the insulator. This latter quantity can be allowed to vary from zero to infinity, thus describing the whole range of compounds from covalent semiconductors to highly insulating materials. We produce an analytical expression of the Schottky-barrier height and of the index of interface behavior, *S*, valid in the whole range of ionicity. *S* is found to fit well the available experimental data. We demonstrate that the capacitor model to estimate *S* is restricted to strongly ionic insulators, while it was generally used in the opposite limit. We suggest finally that the above electronic parameters also drive the strength of adhesion and wetting in nonreactive metal-insulator systems.

I. INTRODUCTION

The understanding of adhesion or wetting of a liquid metal on an insulating material is of crucial interest in a number of technological applications. These include the confinement of liquid metals, which requires highly refractory as well as nonreactive containers: Insulators, or insulating coatings, may be interesting solutions for most of the cases. Moreover, even when noninsulating supports are chosen, their surfaces are generally oxidized at the contact of ambient atmosphere, and become insulating.

It is possible to distinguish two types of adhesion, depending upon the chemical reactivity between the liquid metal and the insulator. Most contacts between metals and very stable oxides with strongly negative free energies of formation (e.g., of alumina, yttria, etc.) are nonreactive or metastable, with very slow rates of reaction. In other cases, a true chemical reaction occurs, and the resulting decrease of interfacial free energy usually yields strong adhesion and a good wetting.¹ Such strong adhesion is sought after in the elaboration of metal-matrix composites² or ceramics brazing alloys, for instance. When the reaction is completed, and thermodynamic equilibrium is reached, the metal is modified by the diffusion of reaction products, and the substrate becomes either the initial insulator covered with adsorbed species, or even a coating of an insulating solid phase pro-

duced by the reaction. However, the new contact is once again nonreactive.

Thus in most instances both types of adhesion merge into the nonreactive one at long times. We focus our attention on this case, for which it is worth noting that important efforts have been made to supply reliable experimental data of wetting angles and adhesion energies, especially on oxides like Al_2O_3 ,³ MgO , and SiO_2 , or carbides¹ like WC , TaC , SiC , or B_4C . These two quantities are related via the Dupré relation, which states that large wetting angles correspond to small adhesion energies. It is possible to sort out the pertinent parameters whose variations are then related to a systematic variation of the adhesion energy: Among these are the value of the Fermi level of the metal, or its electronegativity, and the ionocovalent character of the insulator.^{4,5}

Yet, from a theoretical point of view, most calculations of the adhesion energy W_{adh} are phenomenological. They use either macroscopic thermodynamic quantities to represent the interactions^{3,6} without really explaining the microscopic origin of adhesion, or privilege particular electrostatic interactions like van der Waals forces,¹ image forces⁷ or surface plasmons.⁸ With one exception,⁹ these models do not rely on a true microscopic quantum-mechanical description of the metal-insulator interface. Finally, no real attempt was made, to our knowledge, to include all energetic contributions in calculating W_{adh} : the kinetic surface energy, the electrostatic energy of the

interface dipole, the exchange and correlation contributions, and the short-range core-core repulsion at the solid-liquid interface.

It is our aim to propose a simplified (mostly) analytical microscopic model leading to a realistic evaluation of the adhesion energy. This paper represents the first step in that direction. It describes the modifications of the electronic states at the interface that we think are relevant for understanding W_{adh} . We calculate the electronic structure of a compound insulator of the AB type by a Green's-function method associated with a tight-binding approach. Two possible structures (NaCl rock salt and ZnS zinc blende) are considered, and the ionocovalent character of the insulator is included in a single parameter equal to the ratio of the gap over a hopping energy. Special emphasis is put on the complex dispersion relation at energies in the gap. The insulator electronic states are then matched with metallic free-electron waves at the (100) and (110) surfaces, respectively, for the NaCl and ZnS structures. The density and penetration length of the metallic states induced in the gap (MIGS) of the insulator are calculated, and their dependence upon the metal Fermi energy and the ionocovalent character of the insulator is discussed. This goes beyond previous studies of MIGS proposed in the literature which either were applied to specific metal-semiconductor systems (Al/GaAs, Al/ZnS, and Al/ZnSe by the numerical methods in Refs. 10–12), or made use of a nearly-free-electron picture for small-band-gap semiconductors.^{13,14} Here we are able to calculate the MIGS characteristics for realistic band structures of insulators with various crystal structures. We can also vary the ionocovalent character of the insulator, ranging from covalent semiconductors to highly insulating materials.

We self-consistently determine the Fermi level of the total system by direct and analytical resolution of the Poisson equation. We think that this part represents the most original contribution of our work, compared to previous attempts, performed in the context of metal-semiconductor interfaces. We also give an analytical expression of the Schottky-barrier height and its dependence upon the metal electronegativity, valid in the whole range of ionicity of the insulator, which fits satisfactorily experimental determinations of these quantities. A partial account of this work was already presented in Ref. 15.

We describe in Sec. II the modifications of the electronic structure of an insulator at an interface with a metal. Section III contains the self-consistent determination of the Fermi energy, while Sec. IV deals with a discussion of the Schottky-barrier height.

II. ELECTRONIC STRUCTURE AT THE METAL-INSULATOR INTERFACE

A. Electronic structure of the insulator

We construct in this section a model of the electronic structure of an insulator of the AB type, crystallized in a rock-salt or a zinc-blende structure. We will restrict ourselves to a one-electron Hamiltonian involving a single

orbital per site of energy ε_A for the anions (assumed to lie at Bravais lattice points \mathbf{R}) and ε_C for the cations (located at positions \mathbf{Y} deduced from \mathbf{R} by a translation \mathbf{v}), and a hopping term β for the electrons between neighboring sites:

$$H = \beta \sum_{(\mathbf{R}, \mathbf{Y})} (|A_{\mathbf{R}}\rangle \langle C_{\mathbf{Y}}| + |C_{\mathbf{Y}}\rangle \langle A_{\mathbf{R}}|) + \varepsilon_A \sum_{\mathbf{R}} |A_{\mathbf{R}}\rangle \langle A_{\mathbf{R}}| + \varepsilon_C \sum_{\mathbf{Y}} |C_{\mathbf{Y}}\rangle \langle C_{\mathbf{Y}}|. \quad (2.1)$$

We wish to express the two-dimensional Fourier transform of the Green's function of the insulator $G_E(\mathbf{K}_{\parallel}, z; \mathbf{K}_{\parallel}, z')$, suited to a later study of, respectively, a (100) or a (110) surface. These surfaces have been chosen for their high stability. In this notation of the Green's function, z and z' are the normal components of \mathbf{r} and \mathbf{r}' , and \mathbf{K}_{\parallel} is a two-dimensional (2D) wave vector parallel to the interface. We make use of Bloch theorem to write the wave functions in each energy band ε under the form

$$\psi_{\mathbf{k}}^{\varepsilon}(\mathbf{r}) = e^{i\mathbf{k} \cdot \mathbf{r}} u_{\mathbf{k}}^{\varepsilon}(\mathbf{r}), \quad (2.2)$$

so that $G_E(\mathbf{K}_{\parallel}, z; \mathbf{K}_{\parallel}, z')$ can be expressed as a function of the projections \mathbf{G}_{\parallel} of the reciprocal lattice vectors on the interface and as a function of the group velocity of the electrons at an energy E , under the following form:

$$G_E(\mathbf{K}_{\parallel}, z; \mathbf{K}_{\parallel}, z') \propto \sum_{\mathbf{G}_{\parallel}, k_z^{\varepsilon}(\mathbf{K}_{\parallel} - \mathbf{G}_{\parallel}), \varepsilon} \frac{e^{ik_z^{\varepsilon}(\mathbf{K}_{\parallel} - \mathbf{G}_{\parallel})|z - z'|} [u_{\mathbf{k}}^{\varepsilon}(\mathbf{G}_{\parallel}, z_{<})]^* u_{\mathbf{k}}^{\varepsilon}(\mathbf{G}_{\parallel}, z_{>})}{dE^{\varepsilon}/dk_z(\mathbf{K}_{\parallel} - \mathbf{G}_{\parallel}, k_z^{\varepsilon}(\mathbf{K}_{\parallel} - \mathbf{G}_{\parallel}))}, \quad (2.3)$$

with $z_{>} = \max\{z, z'\}$, $z_{<} = \min\{z, z'\}$, $\mathbf{k} = (\mathbf{K}_{\parallel} - \mathbf{G}_{\parallel}, k_z^{\varepsilon}(\mathbf{K}_{\parallel} - \mathbf{G}_{\parallel}))$. The $k_z^{\varepsilon}(\mathbf{K}_{\parallel} - \mathbf{G}_{\parallel})$ are the poles of the Green's function with a positive imaginary part (i denotes the pole index).

It is proved in the Appendix that, provided that the atomic orbitals are not too much localized on the ions and that energy E under consideration does not approach ε_A or ε_C too closely, $G_E(\mathbf{K}_{\parallel}, z; \mathbf{K}_{\parallel}, z')$ may be approximated by the following expression:

$$G_E(\mathbf{K}_{\parallel}, z; \mathbf{K}_{\parallel}, z') \approx N \sum_{\varepsilon, k_z^{\varepsilon}(\mathbf{K}_{\parallel})} \frac{e^{ik_z^{\varepsilon}(\mathbf{K}_{\parallel})|z - z'|}}{dE^{\varepsilon}/dk_z(\mathbf{K}_{\parallel}, k_z^{\varepsilon}(\mathbf{K}_{\parallel}))}. \quad (2.4)$$

The proportionality coefficient N is determined by using the quantized value of the derivative discontinuity of G_E as z approaches z' .¹³

Of course, the space dependence of G_E is not fully reproduced by such an expression, but nevertheless an important part of the electronic structure is still included in it through the group velocity and the k_z wave vector. This latter is of special importance at energies in the gap of the insulator, since it accounts for the penetration length of electrons.

For both structures that we have chosen, it is straightforward to obtain explicitly the properties of the band

structure, and the expressions of the poles and of the group velocity. Let us just note the following: (1) In this model there is only one conduction band ($\epsilon = +1$) and one valence band ($\epsilon = -1$). (2) The bottom of the conduction band lies at ϵ_C , and the top of the valence band at ϵ_A , so that the minimum value of the gap is $(\epsilon_C - \epsilon_A)$ in both cases. Nevertheless, the gap width depends upon \mathbf{K}_{\parallel} , $(\epsilon_A + \epsilon_C)/2$ being always at the center of the total gap. (3) When E lies in the upper half of the gap [$E > (\epsilon_C + \epsilon_A)/2$], the poles are built from conduction-band states ($\epsilon = 1$), while in the lower half of the gap they come from the valence-band states ($\epsilon = -1$). The center of the gap thus represents a "zero-charge point," E_{ZCP} , which means that the insulator bears a net charge as soon as the Fermi level differs from E_{ZCP} . This concept was introduced in the context of the Schottky barrier, first thanks to a phase-shift approach,¹⁶ which is easy to perform in one-dimensional models. Later it was suggested¹⁷ that this point could be determined by searching the branch point of the complex band structure of the semiconductor for energies inside the gap. This is precisely what we have done.

For the two structures that we have considered, $G_E(\mathbf{K}_{\parallel}, z; \mathbf{K}_{\parallel}, z')$ takes a simple form as a function of the interplane distance d parallel to the interface and of the real and imaginary parts $\pm k_0$ and k_1 of the pole (with $0 \leq k_0 < \pi/d$):

$$G_E(\mathbf{K}_{\parallel}, z; \mathbf{K}_{\parallel}, z') = (m/\hbar^2) \exp(-k_1|z-z'|) \times h(|z-z'|), \quad (2.5)$$

where

$$h(Z) = [\cos(k_0 Z) + \cot(k_0 d) \tanh(k_1 d) \sin(k_0 Z)]/X \quad (2.6)$$

and

$$X = k_0 \cot(k_0 d) \tanh(k_1 d) - k_1 = 1/h(0). \quad (2.7)$$

The important point to note is that all electronic properties of the insulator at midgap can be expressed as a function of only two parameters: one which scales the energies with respect to a fixed one (e.g., the vacuum level), and the second which is the ratio $(\epsilon_C - \epsilon_A)/\beta$ between the gap and the hopping energy. We are thus able with this model to account for the properties of highly insulating materials as well as covalent compound semiconductors by simply letting this parameter vary from infinity to zero. This is not possible when a nearly-free-electron model is used. It will thus happen in the following that we use the terms insulator or semiconductor without distinction to refer to the part of the system that presents a gap.

It is also interesting to compare our complex wave vector with the Franz interpolation¹⁸ used by Feuchtwang *et al.*¹⁹ in the context of the Schottky barrier. The Franz formula is an interpolation between the effective-mass approximations of the penetration length $1/k_1$ close to the valence-band maximum and the conduction-band minimum. At midgap, which represents the position of the Fermi level in the insulator, we find for LiF and BaF₂

that $1/k_1$ given by the Franz law is several times smaller than the one deduced from our model. In our opinion, the calculation of the midgap wave vector requires a coherent description of the entire dispersion law, especially in the case of strongly ionic insulators. As the gap becomes larger, Franz interpolation becomes more and more inaccurate.

B. Electronic structure of the metal-insulator interface

In order to keep the lowest possible number of parameters in our problem, we have chosen to describe the metal by a jellium, whose eigenstates are plane waves. All the metallic characteristics thus depend upon the usual quantity r_s and the position of the bottom of the conduction band E_c with respect to the vacuum level. Let us assume henceforth that the metal lies on the $z < 0$ side of the interface and the insulator lies on its $z > 0$ side. In doing so, we implicitly assume that the interface is abrupt, which may be compatible with a nonreactive adhesion process and possibly with a reactive one at thermodynamical equilibrium. It is well recognized that a simple one-dimensional matching at a given \mathbf{K}_{\parallel} may be achieved, provided that the off-diagonal components $G_E(\mathbf{K}_{\parallel}, z; \mathbf{K}_{\parallel} + \mathbf{g}, z')$ of the Green's function can be neglected with respect to the diagonal ones $G_E(\mathbf{K}_{\parallel}, z; \mathbf{K}_{\parallel}, z')$. We prove in the Appendix that, under the same assumptions as above, the terms $G_E(\mathbf{K}_{\parallel}, z; \mathbf{K}_{\parallel} + \mathbf{g}, z')$ indeed are small as soon as \mathbf{K}_{\parallel} does not lie on a Brillouin-zone edge. Under such circumstances, the electronic wave function in the insulator at a given \mathbf{K}_{\parallel} and energy E is simply proportional to $G_E(\mathbf{K}_{\parallel}, z; \mathbf{K}_{\parallel}, 0)$, given by Eq. (2.5) (this result can be deduced from a general theory of Green's-function matching^{13,20}). We restrict ourselves in the following to energies E lying in the gap, and calculate the amplitude and penetration of a plane wave originating from the metal and vanishing in the insulator.

The matching process involves reflection and transmission coefficients r and t at the interface:

$$r = (iK - X)/(X + iK) \quad (2.8)$$

and

$$t = 2iK/(X + iK), \quad (2.9)$$

with X given by (2.7), and K , the z component of the wave vector at a given \mathbf{K}_{\parallel} in the metal, given by

$$K^2 + \mathbf{K}_{\parallel}^2 = 2m(E - E_c)/\hbar^2. \quad (2.10)$$

The MIGS local density of states $n(E, \mathbf{K}_{\parallel}, z)$ at energy E and parallel wave vector \mathbf{K}_{\parallel} per unit interface area is proportional to the squared amplitude of the wave function. The local density of states $n(E, z)$ per unit interface area follows thanks to a summation over \mathbf{K}_{\parallel} in the 2D first Brillouin zone (BZ). We use the "special points" method first proposed by Chadi and Cohen²¹ for 3D integrals and developed in 2D geometry by Cunningham.²² Our numerical results show that the first- and second-order approximations of this method are not accurate

enough quantitatively and even qualitatively. This implies that it is not possible to use a single special point, which would have allowed us to achieve a complete analytical analysis.

Once the density of states at a given \mathbf{K}_{\parallel} is obtained, all other integrated quantities follow, such as the total density of states $n(E)$, and the local density of states per unit area $n(E, z)$.

C. MIGS density of states

As is usual in these calculations,^{10,13,14} the total density of states $n(E)$ in the insulator at energies in the gap has flat minimum near the middle of the gap, and Van Hove singularities at the gap edges. The type of divergence differs for the NaCl and the ZnS structures. For NaCl, the extrema of the conduction and valence bands are located on a surface of two dimensions in the 2DBZ, and the divergence is an inverse square root of the energy, while for ZnS the same quantity is unidimensional, and the divergence is logarithmic. It should be noticed that a precise description of the band edges requires more special points than anywhere else in the gap, and the validity of the special-point method was checked there. At midgap, we obtain typical values of 7.5×10^{-3} state/eV \AA^2 for the MIGS density of states $n(E)$. This value corresponds to $\epsilon_A - E_c \approx 10$ eV, $\epsilon_C - \epsilon_A = 4$ eV, $\beta = 1.5$ eV, and a lattice parameter $a = 5.41$ \AA , representative of the system Al/ZnS. It can be compared to the results of Louie *et al.*¹⁰ obtained by a self-consistent pseudopotential method on the same system. These authors give a value of 1.4×10^{-2} state/eV \AA^2 for D_s , which denotes the MIGS density of states at midgap $n[(\epsilon_C + \epsilon_A)/2]$: yet, in their calculation, the minimum of $n(E)$ does not occur at midgap; the minimum density of states is of the order of 1.1×10^{-2} state/eV \AA^2 , which is rather close to our value.

The space dependence of the MIGS density of states is represented in Fig. 1 for a ZnS type of interface, and for two typical energy values, one near a band edge and one at the center of the gap. In the first case the oscillating behavior of $n(E, z)$ is weakly damped, and it is clear that the MIGS are gradually transforming into the propagating states expected in the valence or conduction bands. On the opposite, at midgap, the amplitude of the oscillations is small, and the damping of the MIGS is maximum, typically of the order of the interplanar distance in the insulator. It is interesting to note that the overall space dependence of the MIGS density that we find is in agreement with that obtained by Louie *et al.*¹⁰ numerically. This suggests that the simplification of the Green's function that we have made [Sec. II, Eq. (2.4)] preserves the essential characteristics of the local density of states, and it justifies *a posteriori* the use of this approximation.

With the idea of proceeding with analytical calculations in our study of the adhesion energy, we noticed that the dominant feature of $n(E, z)$ at midgap is its exponential decrease; on the opposite, the smallness of the oscillation amplitude makes this latter only a secondary feature, and the simple exponential character is more and more pronounced as $(\epsilon_C - \epsilon_A)/\beta$ increases. For this reason,

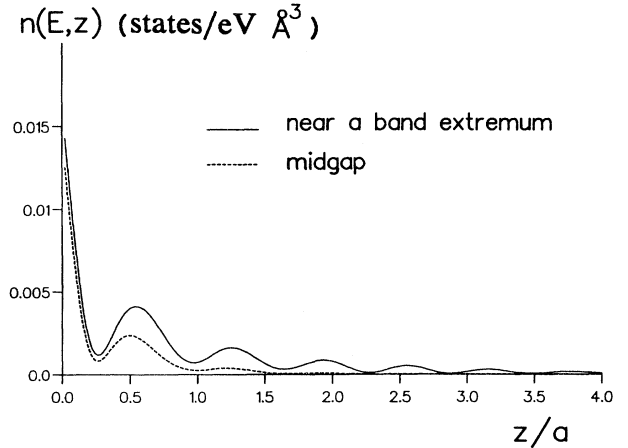


FIG. 1. MIGS local density of states $n(E, z)$ at the interface between a metal and a (110) surface of a semiconductor with a zinc-blende structure using the following set of parameters: $\epsilon_A - E_c = 10$ eV, $\epsilon_C - \epsilon_A = 4$ eV, $\beta = 3$ eV, and the lattice parameter $a = 5$ \AA . $n(E, z)$ was calculated for $E = 0.1$ eV above the valence-band maximum (solid line) and at midgap (dashed line).

we performed an exponential fit of $n(E, z)$ at midgap:

$$n((\epsilon_A + \epsilon_C)/2, z) \approx n_0 \exp(-z/l_p), \quad (2.11)$$

with two parameters: the MIGS density at the interface $n_0 = n((\epsilon_A + \epsilon_C)/2, z=0)$ and the penetration length l_p . Since in our approach the insulator is completely characterized by the ratio $(\epsilon_C - \epsilon_A)/\beta$, we find the important result that n_0 and l_p depend only on the ionocovalent character of the insulator, and on the metal density of states at midgap.

Figures (2a) and (2b) display the variations of n_0 and l_p with $(\epsilon_C - \epsilon_A)/\beta$. It is found that n_0 does not vary strongly with $(\epsilon_C - \epsilon_A)/\beta$, in contrast with the penetration length, which decreases rapidly with increasing ionicity. This can be easily understood because as the gap increases, the electronic waves at midgap lose the propagative character of the conduction and valence states, and thus become more and more damped ($1/l_p$ is roughly proportional to an average value of the imaginary part of the pole wave vector k_1 over the 2DBZ).

On the other hand, n_0 is strongly dependent on the metal density of states because variations of the latter induce large variations of the transmission coefficient t at the interface: n_0 is roughly proportional to $K/(K^2 + X^2)$, and thus presents a maximum at $K \approx X$ and a $1/K$ decrease at large- K values. This behavior appears in Fig. 3, which displays the variations of n_0 versus $\epsilon_A - E_c$ (increasing values of this energy shift imply increasing metal density of states at midgap). By contrast, the dependence of l_p upon $\epsilon_A - E_c$ is very weak, and would be completely vanishing if l_p were calculated with a single special point.

Before concluding this section, it is worth stressing that on the insulating side of the interface, the MIGS represent new available states, compared to those of the isolated insulator. Their appearance is accompanied by a decrease in the number of states in the conduction and

valence bands.^{16,23} When the electrons fill these states, it is found that charge neutrality occurs only if the MIGS are filled up to the zero-charge point discussed previously, which in our model coincides with midgap.

III. SELF-CONSISTENT DETERMINATION OF THE FERMI ENERGY

In order to fully characterize the electronic structure at the metal-insulator interface, it is necessary to self-consistently account for the electric field created by the dipole induced by the electron transfer subsequent to the mismatch between the metal Fermi energy and the zero-charge point of the insulator. To perform this self-consistent procedure, we are helped by the simple analytical form of the local densities of states on both sides of the interface, and we will use a Thomas-Fermi approximation for the screening effects.

Let us call $V(z)$ the electric potential, averaged over the surface, created by a charge distribution $\rho(z)$; $V(z)$ is related to $\rho(z)$ by the Poisson equation

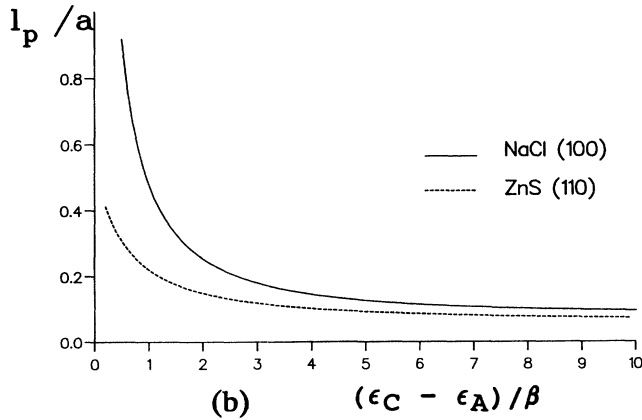
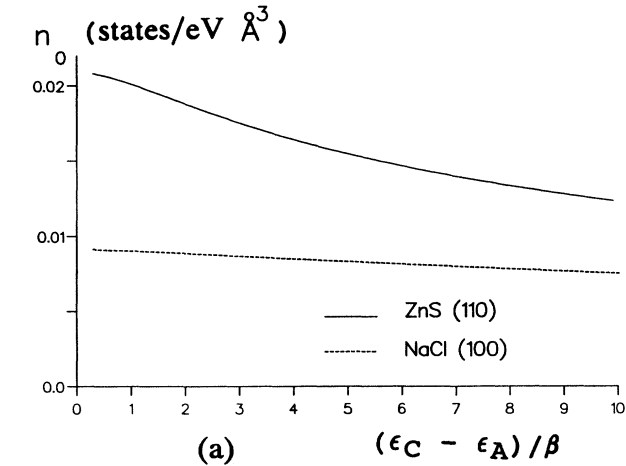


FIG. 2. MIGS local density of states n_0 at the interface (a) and MIGS penetration length l_p (b) at the midgap vs the ratio of the gapwidth to the hopping energy of the insulator for both types of insulator structures and surfaces; the parameter values are $\epsilon_A - E_c = 6$ eV and the lattice parameter $a = 5$ Å.

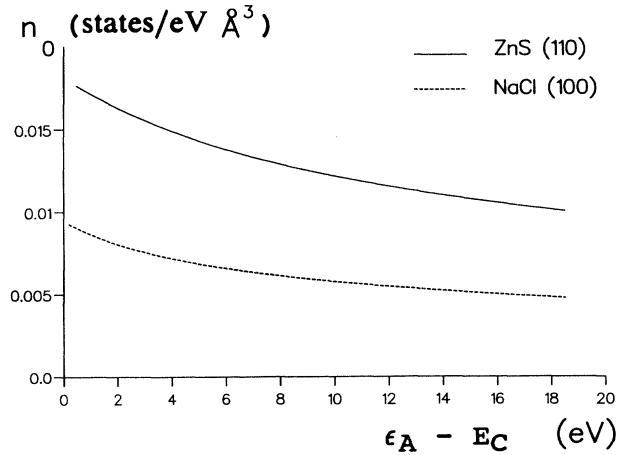


FIG. 3. MIGS local density of states n_0 at the interface and at midgap vs $\epsilon_A - E_c$ for both types of insulator structures and surfaces; the parameter values are $\epsilon_C - \epsilon_A = 5$ eV, $\beta = 1.5$ eV, and the lattice parameter $a = 5$ Å. The dependence of n_0 and l_p upon $\epsilon_A - E_c$ mimics the role of the metal density of states.

$$\frac{d^2V}{dz^2} = -\rho(z)/\epsilon_\alpha. \quad (3.1)$$

ϵ_α is the dielectric constant, equal to ϵ_0 in the metal ($z < 0$) and to $\epsilon_0\epsilon_i$ in the insulator ($z > 0$). Let $n_m(E)$ denote the metal density of states, and E_{ZCP} the point of charge neutrality of the insulator in the absence of any dipole energy shift. In a Thomas-Fermi approximation, the charge density on the metallic side of the interface ($z < 0$) reads

$$\rho(z) \approx -en_m(E_F)[-eV(z)], \quad (3.2)$$

while, on the insulator side ($z > 0$)

$$\rho(z) \approx -en_0 \exp(-z/l_p)[E_F - E_{ZCP} + eV(z)]. \quad (3.3)$$

Two points should be noted. First, it is not necessary to know the modifications of the insulator valence- and conduction-band density of states to calculate $\rho(z)$. Only the departure of the Fermi level from the zero-charge point is relevant, and as a consequence, within a Thomas-Fermi approximation, only the density of MIGS at midgap is required. The second point concerns the similarity in our way of treating the metal and the insulator screening processes, which may seem surprising at first sight. Actually, in a range of distances of the order of l_p from the interface, the MIGS confer a metallic behavior to the insulator, with the possibility of elementary excitations of zero energy. In this space region, the insulator thus possesses two kinds of polarizability: an ionic one, which we account for in the dielectric constant ϵ_i , and a metallic one, a function of the MIGS density.

Due to the simplicity of the space dependence of $\rho(z)$, it is possible to solve exactly the Poisson equation for this system. We introduce l_m and l_i , equal, respectively, to the metal and insulator Thomas-Fermi lengths:

$$l_m = [\epsilon_0/e^2 n_m(E_F)]^{1/2}, \quad (3.4)$$

$$l_i = (\epsilon_0 \epsilon_i / e^2 n_0)^{1/2}. \quad (3.5)$$

Let α and α' denote two matching coefficients, and $I_0(x)$ and $I_1(x) = I_0'(x)$ the two first modified Bessel functions;²⁴ the general solution for the potential on both sides of the interface is the following:

$$V(z) = (E_{ZCP} - E_F)/e + \alpha I_0(2l_p \exp(-z/2l_p)/l_i), \quad z > 0, \quad (3.6)$$

$$V(z) = \alpha' \exp(z/l_m), \quad (z < 0) \quad (3.7)$$

which straightforwardly yields for $z > 0$

$$eV(z) = (E_{ZCP} - E_F) \times \left[1 - \frac{I_0(2l_p \exp(-z/2l_p)/l_i)}{I_0(2l_p/l_i) + (l_m/l_i)\epsilon_i I_1(2l_p/l_i)} \right]. \quad (3.8)$$

The potential $V(z)$ is induced by the perturbing potential $(E_{ZCP} - E_F)$ via screening effects. A quick inspection of the results shows that the two limiting cases where the MIGS density n_0 is either very large or very small indeed have the expected behavior: in the first case, achieved for covalent semiconductors, l_p/l_i goes to $+\infty$, and the screening processes are very efficient; the induced potential is equal to the external one. The Fermi level is pinned at the position of the zero-charge point of the insulator. In the other limit where few MIGS are available, the screening is inefficient: the induced potential is close to zero. The Fermi level of the system is imposed by the metal, and can lie anywhere in the insulator gap. Equation (3.8) provides an analytical expression for the potential valid for any value of the MIGS density lying between these two limits (Fig. 4). It should be noted, that, up to now, no such analytical self-consistent determination of the Fermi level has been proposed in the literature, to our knowledge. There exist numerical resolutions, by means of the self-consistent pseudopotential method, for instance.¹⁰⁻¹² There exists also a model in which the dipole is approximated by a planar capacitor, the positive charge and the negative charge being localized at a distance from the interface of the order of screening length.²⁵ We will come back to this point in the following section.

Moreover, it appears in our calculation that a precise determination of E_F relies on a good knowledge of $1/k_1$ at midgap. For such an energy, we have proved in Sec. II A that the effective-mass approximation involved in the Franz formula¹⁸ is increasingly inaccurate as the gap increases. It was thus important to make a realistic model of the dispersion relation of the insulator.

Up to this point, we have made a thorough description of the metal-insulator interface, with special emphasis on the metallic states induced in the gap of the insulator, and on the location of the Fermi energy. This represents the first step in our study of the adhesion energy of liquid metals on insulators. The calculation of the various energy contributions is postponed to a following paper. Yet,

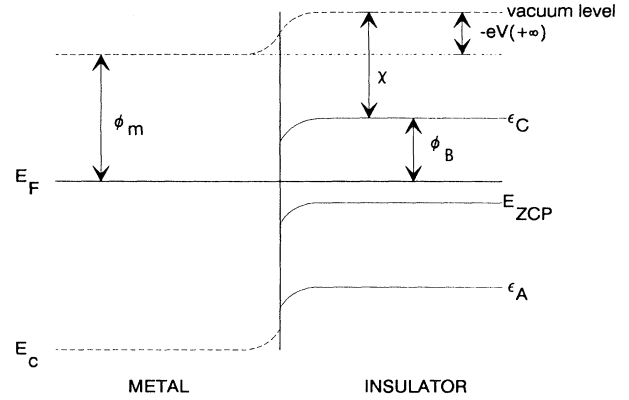


FIG. 4. Local distortions of the metal and insulator band structures induced by the interface dipole potential. The Fermi level remains constant in all space.

since our model of the insulator allows us to consider the whole range of ionicity, we have reconsidered the problem of the Schottky-barrier height, popular in the field of metal semiconductor junctions. It is presented in the next section.

IV. THE SCHOTTKY-BARRIER HEIGHT

The first model accounting for the barrier height Φ_B between a metal and a semiconductor goes back to Schottky,²⁶ who proposed that the energy necessary to excite an electron from the metal Fermi level E_F to the bottom of the semiconductor conduction band is simply equal to the difference between the metal work function Φ_m and the semiconductor affinity (Fig. 4). Later experiments proved that this law was not obeyed for most of the existing contacts, and this led Bardeen²⁷ to propose that intrinsic surface states of the semiconductor provided a large density of state in the gap, which pinned the Fermi level at the surface states energy: under such circumstances, Φ_B becomes independent of the metal electronegativity, as observed in a number of systems. The Schottky and Bardeen models represent two extreme situations, which apply, respectively, to highly insulating and very covalent semiconductor-metal junctions. They were later developed and gave birth to the two families of approached now existing in this field, namely the induced density of interface states model and the defect model (for a review, see, e.g., Refs. 28-31). Considering our model of the interface, we will be only able here to compare our results with the first family, which suits to a perfect and abrupt contact between a thick metallic overlayer and a semiconductor.

The induced density of interface states model stresses the importance of the MIGS in fixing the barrier height Φ_B . With our notations (cf. Fig. 4), Φ_B is simply related to the Fermi energy, the bottom of the conduction-band energy ϵ_C (in the absence of any dipole shift), and the electrical potential $V(z)$

$$\Phi_B = \epsilon_C - E_F - eV(+\infty), \quad (4.1)$$

which assumes that deep inside the metal there is no macroscopic charge [$V(-\infty)=0$].

When a covalent semiconductor is involved in the junction, the density of MIGS is large, so that $E_F = E_{ZCP} - eV(+\infty)$. The Schottky barrier becomes independent of the characteristics of the metal used for the junction:

$$\Phi_B^{sc} = \epsilon_C - E_{ZCP}, \quad (4.2)$$

("sc" standing for "screened") because the Fermi level is pinned at the zero-charge point. A number of numerical studies, most of them using the pseudopotential method, have satisfactorily described this limit, achieving^{16,10,12,32,33} or not achieving^{23,34,35} the self-consistent procedure.

When the ionic character of the semiconductor increases, the density of MIGS decreases and can no longer screen the difference between E_F and E_{ZCP} . A proper consideration of screening effects is thus necessary to account for the large variations of position of the Fermi level in the gap. Indeed, only the numerical calculations that included the self-consistency¹⁰⁻¹² were able to reproduce the variation S of the Schottky-barrier height as a function of the electronegativity of the metal,^{36,37} while the non-self-consistent approaches³⁵ concluded that many-body effects were perhaps responsible for the observed behavior. Restricted to the very ionic limit, a self-consistent analytical approach was also performed¹⁹ to interpret experiments on LiF and BaF₂. In the extreme ionic limit, the Schottky barrier becomes equal to the value proposed by Schottky ("uns" standing for "un-screened"):

$$\Phi_B^{uns} = \epsilon_C - E_F. \quad (4.3)$$

Compared to these studies, our approach has the advantage of giving an analytical expression for Φ_B valid in the whole range of ionicity of the semiconductor, based upon a microscopic description of the states at the interface. It is, in spirit, similar to that of Feuchtwang,¹⁹ but our calculation of the charge density at the interface is more general than his, which makes use of the Franz approximation¹⁸ for the insulator, and which is valid only when a very small density of MIGS exists. Moreover, this author, following a model by Cowley and Sze,²⁵ assumes that the charge density can be approximated by a capacitor with an *ad hoc* thickness, while we have been able, for the first time, to integrate the Poisson equation. Consequently, instead of writing an interpolation of the type

$$\Phi_B = \Phi_B^{uns}/w + \Phi_B^{sc}(1-1/w) \quad (4.4)$$

with a phenomenological parameter w such that $0 < 1/w < 1$, we are able to reach a similar expression and to assign to w the meaning of an effective dielectric constant:

$$w = I_0(2l_p/l_i) + \epsilon_i(l_m/l_i)I_1(2l_p/l_i). \quad (4.5)$$

We can also write down an analytical expression for the

index of interface behavior S which is the derivative of the Schottky-barrier height with respect to the metal electronegativity:

$$S = A/w. \quad (4.6)$$

Equation (4.6) was obtained by deriving the factor $(E_F - E_{ZCP})$ in $V(z)$ with respect to the metal electronegativity X_m (A denotes $-dE_F/dX_m$). On the other hand, we have neglected the dependence of w upon X_m , which gives corrections smaller than 10%. Equations (4.5) and (4.6) are interesting because they can be compared to the one derived from the model of Cowley and Sze:²⁵

$$S = A/(1 + e^2 D_s l_{eff}/\epsilon_0). \quad (4.7)$$

In this equation, D_s is the density of interface states, and l_{eff} is the effective thickness of the capacitor. l_{eff} is generally evaluated as the sum of a metallic length (the Thomas-Fermi screening length divided by a metallic dielectric constant) plus a semiconducting one (the interatomic distance or mean penetration length of the MIGS from Louie *et al.*,¹⁰ divided by the semiconductor dielectric constant). Our general expression [Eq. (4.5)] yields (4.7) only in a limiting case, namely when the ionic character of the insulator is large. In that case the ratio l_p/l_i goes to zero and it is licit to perform a polynomial development of the Bessel functions to lowest order. We find

$$S \approx \frac{A}{1 + \epsilon_i(l_p/l_i^2)(l_p/\epsilon_i + l_m)}. \quad (4.8)$$

Equation (4.8) is equivalent to (4.7) because $D_s = n(\epsilon_C + \epsilon_A)/2 = n_0 l_p$, which is found by integrating Eq. (2.11) over z , and because $n_0 l_p = \epsilon_0 \epsilon_i l_p / (el_i)^2$.

However, when the ionic character of the insulator decreases, the approximate form of S (4.7) gets increasingly less accurate: we find that the relative error on S is of the order of 5% for MgO, 30% for ZnS, and 200% for GaAs (the approximate form being overevaluated). This happens because in the semiconductor there is a competition between two characteristic lengths in limiting the MIGS penetration: l_p , the MIGS damping length, and l_i , the MIGS metallic screening length. In the ionic limit, l_p is much smaller than l_i , and thus l_p is the correct length to consider. However, in the other limit, in which, unfortunately, (4.7) was mostly used, l_i limits the charge penetration instead of l_p . An approximate expression for S can still be derived that makes use of the asymptotic form of the Bessel functions when $l_p/l_i \gg 1$:

$$S \approx A(4\pi l_p/l_i)^{1/2} \exp(-2l_p/l_i)/(1 + \epsilon_i l_m/l_i). \quad (4.9)$$

Another interesting feature in the expressions (4.5) and (4.6) of S is that all characteristics of the "semiconductor" are included in the ratio $(\epsilon_C - \epsilon_A)/\beta$. There has been a debate in the literature concerning the pertinent way of representing the variations of S for various semiconductors. Most of the authors followed the compilation of experimental data performed by Kurtin and McGill,³⁶ which was done as a function of the electronegativity difference $(X_A - X_C)$ between the anions and cations of the semiconductor. One of the reasons was the

striking behavior of S in this representation, which seemed to reveal an abrupt separation between covalent semiconductors and ionic ones. Later, Schlüter³⁷ reanalyzed the experimental data with their error bars, and concluded that the transition was actually very smooth. Cohen³⁸ stressed that $(X_A - X_C)$ was not the pertinent parameter because a semiconductor with a single type of atoms, like diamond, had a nonzero S value. He proposed to use instead the product of the gap times the surface cell area. Actually, our pertinent parameter $(\epsilon_C - \epsilon_A)/\beta$ is very close to the latter, considering that a good order of magnitude of the hopping integrals is given by Harrison's empirical law³⁹⁻⁴¹ in one over the squared interatomic distance.

We have represented in Figs. 5(a) and 5(b) the variations of S versus $(\epsilon_C - \epsilon_A)/\beta$ for a NaCl(100) and a ZnS(110) type of interface and three positions of the Fermi level corresponding typically to one, two, and three valence electrons per atom in the metal. We have taken a value of 1 for ϵ_i to obtain these curves because the penetration length at midgap is in all cases smaller than the interatomic distance, so that the ionic polarizability is not very efficient. Louie *et al.*¹⁰ justified the use of $\epsilon_i = 2$ for GaAs and Si with the argument that the penetration

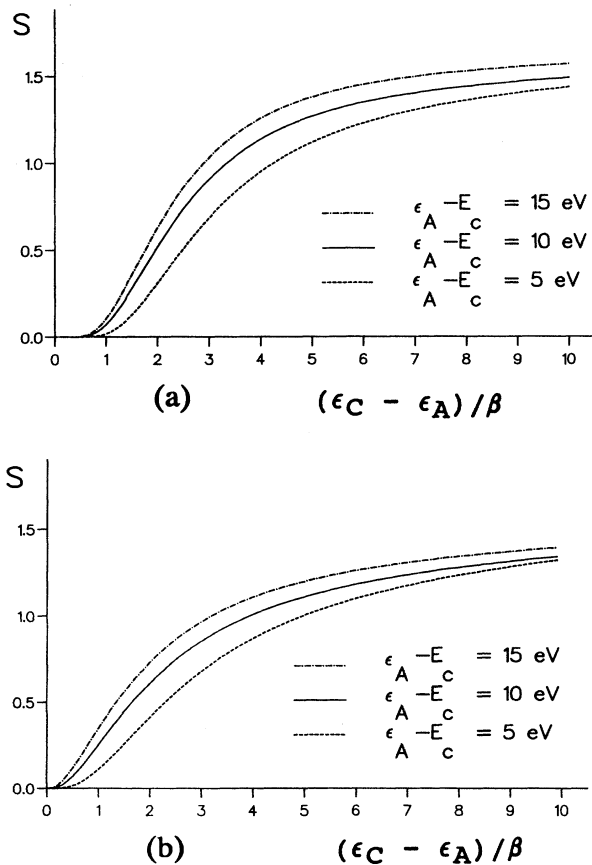


FIG. 5. Index of interface behavior S (in eV) as a function of the ratio $(\epsilon_C - \epsilon_A)/\beta$ of the gapwidth over the insulator hopping energy for NaCl(100) (a) and ZnS(110) (b) types of surfaces and for typical values of the parameter $\epsilon_A - E_c$.

length averaged over the gap was equal to 2.8 and 3 Å, respectively. Since the relevant l_p at midgap is several times smaller than the averaged one, we found that $\epsilon_i = 1$ was a better compromise.

S increases continuously from $S = 0$, in the most covalent case, to a maximum value theoretically equal to A , but which hardly exceeds $A/2$ for realistic values of the ratio $(\epsilon_C - \epsilon_A)/\beta$ [we have taken $A = 2.9$ in Figs. 5 and 6 since work-function data yield a value of A ranging from 2 to 3 (Ref. 19)]. This is the order of magnitude experimentally found in LiF and BaF₂,⁴² and also evaluated by Cohen for a hypothetical extremely ionic compound with a gap equal to 20 eV.

We find that the increase of S with the density of metallic electrons is very weak due to the slow variation of the MIGS density with this quantity. We also find that the crystallographic structure of the semiconductor induces only small changes in S [Figs. 5(a) and 5(b)]. An average curve can thus be defined that can be compared with the experimental values.

Figure 6 represents that average theoretical S curve that we obtain, superimposed on the experimental points as compiled by Schlüter,³⁷ Kurtin and McGill,³⁶ and Paudyal and Pong.⁴² It should be kept in mind that in most cases the experimental error bar was estimated at 20%, which is also the order of magnitude of the variations of S with the metal and the crystallographic structure. We have not reported the data on diamond, silicium, and germanium, which cannot be accounted for by our model. The overall agreement is good, better than we would have expected, considering the crudeness in the description of the semiconductor (a single orbital per site, while all compounds at least involve s and p orbitals). This may mean that the Schottky-barrier height depends upon integrated quantities of the band structure rather than upon tiny details of this latter. In that sense it shares this property

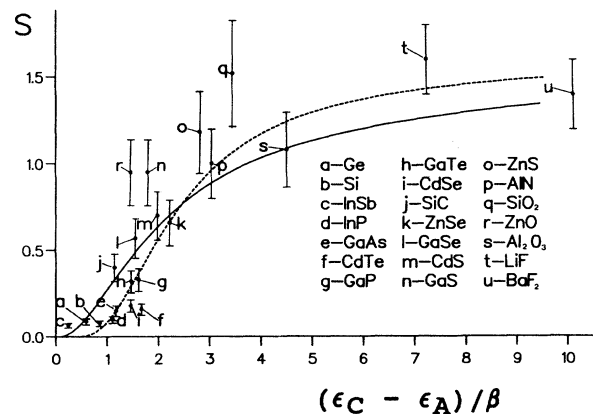


FIG. 6. Index of interface behavior S (in eV) as a function of the ratio $(\epsilon_C - \epsilon_A)/\beta$ of the gapwidth over the insulator hopping energy. Solid and dashed lines are the present theoretical estimates for ZnS(110) (solid line) and NaCl(100) (dashed line) surfaces, calculated for an average electron density in the metal ($\epsilon_A - E_c = 10$ eV). We have reported experimental values found in the literature (Refs. 36, 37, and 42) with their error bars.

with surface energies (the first models of surface energies of transition metals assumed a rectangular density of states) and this is encouraging for our future evaluation of the adhesion energy of liquid metals on insulators.

V. CONCLUSION

We have made a quasianalytical model of a metal-insulator perfect and abrupt interface in order to study nonreactive adhesion processes of liquid metals on insulators. This paper represents the first part of this study. It deals with the description of the electronic states at the interface, and we postpone the evaluation of the energy contributions to the adhesion energy to a forthcoming paper.

The insulator electronic structure is modeled by a tight-binding approach in which a single nondegenerated atomic orbital per anion and per cation is considered. Two crystal structures were accounted for: the NaCl rock-salt and the ZnS zinc-blende ones. We focused our interest on the complex band structure for energies inside the gap, and showed that for both structures the zero-charge point was at midgap.

We performed a matching procedure between the insulator states and free-electron waves characterizing a jellium, at the (100) and (110) surfaces, respectively, most stable for the NaCl and ZnS structures. For energies inside the gap, our quasianalytical description of the MIGS is in good agreement with numerical estimates obtained by the pseudopotential method. At midgap, we characterized the MIGS by two parameters: the density of MIGS at the interface, and the penetration length, and we studied the variations of these parameters with the metal Fermi energy and the insulator ionocovalent character. Letting the ionocovalent character vary from zero to infinity allows a description of a whole range of interfaces: from the covalent semiconductor-metal interface to the highly insulating material-metal interfaces.

Then we performed a self-consistent analytical resolution of the Poisson equation, thanks to a Thomas-Fermi description of the screening processes. The position of the Fermi level was thus obtained, in an analytical way, not only in the limiting cases of very large or very small densities of MIGS, but also in the whole range of values between these two limits. This represents considerable progress compared to the phenomenological capacitor model generally used in this field.

Although this was not our purpose in undertaking this study, we were able at that point to give an analytical expression for the Schottky-barrier height Φ_B and the index of interface behavior S , and describe quantitatively how these quantities depend upon the ionocovalent character of the semiconductor, on the metal Fermi energy, on the crystallographic structure, etc. Our results are in good qualitative agreement with experimental data compiled in the literature. They also allow a discussion of the limit of validity of the capacitor model, which turns out to be restricted to the highly ionic limit. This was not the limit in which it was generally applied. The highest attainable values of S that we find hardly reach half the Schottky limit, in good agreement with experimental as well as pre-

vious theoretical estimates.

Finally, concerning the problem of adhesion and wetting of nonreactive metal-insulator flat and defectless interfaces, our work yields two conclusions:

(i) It first shows that in such systems, for which adhesion and wetting processes are mostly of electronic nature (no interdiffusion), the depth of interaction is determined by the interface modifications of the electronic structures and thus is of the order of the penetration length of the MIGS averaged over the gap. In the case of strongly ionic insulators, this length is a small portion of the distance between two neighboring atomic planes of the insulator parallel to the interface, while it becomes of the same order of magnitude for highly covalent semiconductors. It can never exceed this typical distance.

(ii) Furthermore, the three electronic energetic contributions to the metal-insulator interface energy (the kinetic, electrostatic, and exchange and correlation ones) are principally driven, as well as all the other electronic properties that we have previously discussed, by the value of the Fermi energy of the metal with respect to a reference energy, and by the ratio $(\epsilon_C - \epsilon_A)/\beta$, which represents the ionic character of the insulator. Moreover, we have proved that the electronic properties of such interfaces do not depend much upon either the crystallographic structure of the insulator, or upon the orientation of the interface, and it is encouraging to notice that this is also true for wetting angles and adhesion energies.

ACKNOWLEDGMENTS

We are grateful to Dr. A. Pattoret for constant encouragement during the course of this work, and also to Professor P. Hicter, Professor N. Eustathopoulos, and Dr. D. Chatain for helpful and stimulating discussions about this topic.

APPENDIX

We derive in this appendix a simplified expression for the insulator Green's function, valid when atomic orbitals on anions and cations have a reasonable overlap, with an accuracy of a few percent at midgap. We also show that under the same conditions, $G_E(\mathbf{K}_\parallel, z; \mathbf{K}_\parallel + \mathbf{g}, z')$ is small with respect to $G_E(\mathbf{K}_\parallel, z; \mathbf{K}_\parallel, z')$, \mathbf{g} denoting a vector of the 2D reciprocal lattice.

In a tight-binding approach, with one atomic orbital by anion [$A(\mathbf{r})$] or cation [$C(\mathbf{r})$], the Bloch functions $u_{\mathbf{k}}^{\epsilon}(\mathbf{r})$ [cf. Eq. (2.2)] can be expressed as

$$u_{\mathbf{k}}^{\epsilon}(\mathbf{r}) = \sum_{\mathbf{R}} e^{i\mathbf{k} \cdot (\mathbf{R} - \mathbf{r})} \Phi_{\mathbf{k}}^{\epsilon}(\mathbf{r} - \mathbf{R}), \quad (\text{A1})$$

with

$$\Phi_{\mathbf{k}}^{\epsilon}(\mathbf{r}) = \alpha_{\mathbf{k}}^{\epsilon} A(\mathbf{r}) + \tau_{\mathbf{k}}^{\epsilon} C(\mathbf{r} - \mathbf{v}). \quad (\text{A2})$$

Symmetry arguments valid for the two crystallographic structures under consideration show that $(\mathbf{K}_\parallel - \mathbf{G}_\parallel, k_z^{\epsilon}(\mathbf{K}_\parallel - \mathbf{G}_\parallel))$ differs from $(\mathbf{K}_\parallel, k_z^{\epsilon}(\mathbf{K}_\parallel))$ only by a vector of the 3D reciprocal lattice. Since coefficients $\alpha_{\mathbf{k}}^{\epsilon}$ and $\tau_{\mathbf{k}}^{\epsilon}$ and $dE^{\epsilon}(\mathbf{k})/dk_z$ have the \mathbf{k} periodicity of the 3D reciprocal lattice, one can prove that the sum over \mathbf{G}_\parallel in-

volved in Eq. (2.3) can be achieved, and that this sum can be restricted to the poles $k_z^{ei}(\mathbf{K}_{\parallel})$ with a real part ranging from $-\pi/d$ to π/d (the addition of $2\pi j/d$ to k_z , where d is the interplanar distance parallel to the interface, leaves the current term of the series invariant). Consequently

$$G_E(\mathbf{K}_{\parallel}, z; \mathbf{K}_{\parallel}, z') \propto \sum_{\epsilon, k_z^{ei}(\mathbf{K}_{\parallel})} \frac{e^{ik_z^{ei}(\mathbf{K}_{\parallel})|z-z'|} S_{\mathbf{k}}^{\epsilon}(z_{>}) [S_{\mathbf{k}}^{\epsilon}(z_{<})]^*}{dE^{\epsilon}/dk_z(\mathbf{K}_{\parallel}, k_z^{ei}(\mathbf{K}_{\parallel}))}, \quad (\text{A3})$$

where $\mathbf{k} = (\mathbf{K}_{\parallel}, k_z^{ei}(\mathbf{K}_{\parallel}))$ and

$$S_{\mathbf{k}}^{\epsilon}(z) = \sum_p e^{ik_z^{ei}(\mathbf{K}_{\parallel})(pd-z)} \Phi_{\mathbf{k}}^{\epsilon}(\mathbf{K}_{\parallel}, z-pd). \quad (\text{A4})$$

p denotes an integer in this equation. The p summation in real space may be replaced by a q summation (q denoting an integer) in reciprocal space by introducing the $\Phi_{\mathbf{k}}$ Fourier transform

$$S_{\mathbf{k}}^{\epsilon}(z) \propto \sum_q S_{\mathbf{k}}^{\epsilon q}(z), \quad (\text{A5})$$

where

$$S_{\mathbf{k}}^{\epsilon q}(z) = e^{2\pi i q z/d} \Phi_{\mathbf{k}}^{\epsilon}(\mathbf{K}_{\parallel}, k_z^{ei}(\mathbf{K}_{\parallel}) + 2\pi q/d). \quad (\text{A6})$$

Since $\Phi_{\mathbf{k}}^{\epsilon}(\mathbf{k}')$ decreases at large $|\mathbf{k}'|$ values, the largest term of the sum is the $q=0$ one, which corresponds to the minimum length of $\mathbf{K}_{\parallel}, k_z^{ei}(\mathbf{K}_{\parallel}) + 2\pi q/d$. Keeping only this term in the sum yields simply Eq. (2.4).

We now prove that the accuracy of this approximation is increasingly better as the atomic orbitals $A(\mathbf{r})$ and $C(\mathbf{r})$ have a wider extension. We suppose that the atomic wave functions are Gaussian functions with the same width σ :

$$A(\mathbf{r}) = C(\mathbf{r}) \propto \exp(-r^2/2\sigma^2). \quad (\text{A7})$$

σ must be of the order of half the nearest-neighbor distance to yield a hopping energy β of the order of 1 eV; we

keep this value of σ in the following discussion. The ratio of the q th term over the $q=0$ one is equal to

$$|S_{\mathbf{k}}^{\epsilon q}/S_{\mathbf{k}}^{\epsilon 0}| = \exp[-8\pi^2(\sigma/d)^2 q(q \pm k_0 d/\pi)], \quad (\text{A8})$$

where $\pm k_0$ are the real parts of the poles and $0 \leq (k_0 d/\pi) < 1$. It is very quickly vanishing with increasing $|q|$. However, it is of the order of 1, for $q = \pm 1$, as soon as $k_0 \pi/d$ approaches 1, which happens only when the energy E approaches the gap edges. This is not the range in which we are primarily interested. At midgap, we calculate that in the most unfavorable conditions (a very covalent semiconductor, and with \mathbf{K}_{\parallel} near the edge of the BZ), $|S_{\mathbf{k}}^{\epsilon, q=\pm 1}/S_{\mathbf{k}}^{\epsilon 0}|$ is around 4% for the NaCl structure and 1% for the ZnS structure. Other terms are completely negligible. The conclusion is that approximation (2.4) is rather accurate, especially at midgap.

Under the same conditions, the off-diagonal components of the 2D Fourier transform of the Green's function can be written

$$\frac{|G_E(\mathbf{K}_{\parallel}, z; \mathbf{K}_{\parallel} + \mathbf{g}, z')|}{|G_E(\mathbf{K}_{\parallel}, z; \mathbf{K}_{\parallel}, z')|} = \exp[-2\sigma^2(|\mathbf{K}_{\parallel} + \mathbf{g}|^2 - |\mathbf{K}_{\parallel}|^2)]. \quad (\text{A9})$$

Equation (A9) prove that we can disregard all $G_E(\mathbf{K}_{\parallel}, z; \mathbf{K}_{\parallel} + \mathbf{g}, z')$ terms ($\mathbf{g} \neq 0$) with respect to $G_E(\mathbf{K}_{\parallel}, z; \mathbf{K}_{\parallel}, z')$ as soon as \mathbf{K}_{\parallel} does not approach a BZ edge. Indeed, no special point used in the \mathbf{K}_{\parallel} summation is located on the BZ edges. In order to estimate more quantitatively the accuracy of this approximation, we calculate the ratio (A9) in the case of a single special point, and with σ of the order of the half-nearest-neighbor distance. We find that the maximum value of this ratio is of the order of 0.7% for the NaCl structure and 14% for the ZnS structure.

Summing up all these results shows that the MIGS density at midgap is obtained with an accuracy of better than 5% (the NaCl structure) and 15% (the ZnS structure).

¹Ju. V. Naidich, Prog. Surf. Mem. Sci. **14**, 353 (1981).

²F. Delannay, L. Froyen, and A. Deruyttere, J. Mater. Sci. **22**, 1 (1987).

³D. Chatain, I. Rivollet, and N. Eustathopoulos, J. Chim. Phys. **83**, 561 (1986).

⁴V. Laurent, Ph.D. thesis, Institut National Polytechnique de Grenoble, France (1988).

⁵G. Bordier and C. Noguera, in *Interfaces in New Materials* (Elsevier, London, in press).

⁶J. E. McDonald and J. G. Eberhart, Trans. Metall. Soc. AIME **233**, 512 (1965).

⁷P. W. Tasker and A. M. Stoneham, J. Chim. Phys. **84**, 149 (1987).

⁸A. M. Stoneham, Appl. Surf. Sci. **14**, 249 (1982).

⁹P. Hicter, D. Chatain, A. Pasturel, and N. Eustathopoulos, J. Chim. Phys. **85**, 941 (1988).

¹⁰S. G. Louie, J. R. Chelikowski, and M. L. Cohen, J. Vac. Sci. Technol. **13**, 790 (1976).

¹¹S. G. Louie and M. L. Cohen, Phys. Rev. Lett. **35**, 866 (1975).

¹²S. G. Louie, J. R. Chelikowski, and M. L. Cohen, Phys. Rev. B **15**, 2154 (1977).

¹³F. García-Moliner and F. Flores, *Introduction to the Theory of Solid Surfaces* (Cambridge University Press, London, 1979).

¹⁴V. Heine, Phys. Rev. **138**, A1689 (1965).

¹⁵G. Bordier and C. Noguera, Surf. Sci. **251/252**, 457 (1991).

¹⁶F. Yndurain, J. Phys. C **4**, 2849 (1971).

¹⁷J. Tersoff, Phys. Rev. Lett. **52**, 465 (1984).

¹⁸W. Franz, in *Handbuch der Physik*, edited by H. Geigerand and K. Scheel (Springer, Berlin, 1956) Vol. 17, p. 165.

¹⁹T. E. Feuchtwang, D. Paudyal, and W. Pong, Phys. Rev. B **26**, 1608 (1982).

²⁰F. García-Moliner and J. Rubio, Proc. R. Soc. London, Ser.

- A 324, 257 (1971).
- ²¹D. J. Chadi and M. L. Cohen, *Phys. Rev. B* **8**, 5747 (1973).
- ²²S. L. Cunningham, *Phys. Rev. B* **10**, 4988 (1974).
- ²³C. Tejedor, C. Flores, and E. Louis, *J. Phys. C* **10**, 2163 (1977).
- ²⁴M. Abramowitz and I. Stegun, in *Handbook of Mathematical Functions*, edited by M. Abramowitz and I. Stegun (Dover, New York, 1970), p. 374.
- ²⁵A. M. Cowley and S.M. Sze, *J. Appl. Phys.* **36**, 3212 (1963).
- ²⁶W. Schottky, *Z. Phys.* **113**, 367 (1939).
- ²⁷J. Bardeen, *Phys. Rev.* **71**, 717 (1947).
- ²⁸E. H. Rhoderick, *Metal-Semiconductor Contacts* (Clarendon, Oxford, 1978).
- ²⁹M. Schlüter, *Thin Solid Films* **93**, 3 (1982).
- ³⁰L. J. Brillson, *Surf. Sci. Rep.* **2**, 123 (1982).
- ³¹F. Flores and C. Tejedor, *J. Phys. C* **20**, 145 (1987).
- ³²H. I. Zhang and M. Schlüter, *Phys. Rev. B* **18**, 1923 (1978).
- ³³F. Guinea, J. Sanchez Dehesa, and F. Flores, *J. Phys. C* **16**, 6499 (1983).
- ³⁴F. Flores, E. Louis, and F. Yndurain, *J. Phys. C* **6**, L465 (1973).
- ³⁵E. Louis, F. Yndurain, and F. Flores, *Phys. Rev. B* **13**, 4408 (1976).
- ³⁶S. Kurtin and T. C. McGill, *Phys. Rev. Lett.* **22**, 1433 (1969).
- ³⁷M. Schlüter, *Phys. Rev. B* **17**, 5044 (1978).
- ³⁸M. L. Cohen, *J. Vac. Sci. Technol.* **16**, 1135 (1979).
- ³⁹W. A. Harrison, *Electronic Structures and Properties of Solids* (Freeman, San Francisco, 1980).
- ⁴⁰W. A. Harrison, *Phys. Rev. B* **24**, 5835 (1981).
- ⁴¹W. A. Harrison, *Phys. Rev. B* **31**, 2121 (1985).
- ⁴²W. Pong and D. Paudyal, *Phys. Rev. B* **23**, 3085 (1981).